OXFORD

Cerebral Cortex, 2022, **32**, 4857–4868
https://doi.org/10.1093/cercor/bhab520
Advance access publication date 25 January 2022
Original Article

Brain functional network abnormalities in Parkinson's disease with mild cognitive impairment

Xueling Suo[1,2,3], Du Lei[4], Nannan Li[5], Jiaxin Peng[5], Chaolan Chen[5], Wenbin Li[1], Kun Qin[1], Graham J. Kemp[6], Rong Peng[5,*], Qiyong Gong[1,7,*]

[1]Huaxi MR Research Center (HMRRC), Department of Radiology, West China Hospital of Sichuan University, Chengdu, Sichuan 610041, China,
[2]Research Unit of Psychoradiology, Chinese Academy of Medical Sciences, Chengdu, Sichuan 610041, China,
[3]Functional and Molecular Imaging Key Laboratory of Sichuan Province, West China Hospital of Sichuan University, Chengdu, Sichuan 610041, China,
[4]Department of Psychiatry and Behavioral Neuroscience, University of Cincinnati, Cincinnati, OH 45227, USA,
[5]Department of Neurology, West China Hospital of Sichuan University, Chengdu, Sichuan 610041, China,
[6]Liverpool Magnetic Resonance Imaging Centre (LiMRIC) and Institute of Life Course and Medical Sciences, University of Liverpool, Liverpool L69 3GE, UK,
[7]Department of Radiology, West China Xiamen Hospital of Sichuan University, Xiamen, Fujian 361022, China

*Address correspondence to Rong Peng, Department of Neurology, West China Hospital, Sichuan University, No. 37 Guo Xue Xiang, Chengdu, Sichuan 610041, China. Email: qrongpeng@126.com; Qiyong Gong, Department of Radiology, West China Xiamen Hospital of Sichuan University, Xiamen, Fujian 361022, China. Email: qiyonggong@hmrrc.org.cn

Mild cognitive impairment in Parkinson's disease (PD-M) is related to a high risk of dementia. This study explored the whole-brain functional networks in early-stage PD-M. Forty-one patients with PD classified as cognitively normal (PD-N, $n = 17$) and PD-M ($n = 24$) and 24 demographically matched healthy controls (HC) underwent clinical and neuropsychological evaluations and resting-state functional magnetic resonance imaging. The global, regional, and modular topological characteristics were assessed in the brain functional networks, and their relationships to cognitive scores were tested. At the global level, PD-M and PD-N exhibited higher characteristic path length and lower clustering coefficient, local and global efficiency relative to HC. At the regional level, PD-M and PD-N showed lower nodal centrality in sensorimotor regions relative to HC. At the modular level, PD-M showed lower intramodular connectivity in default mode and cerebellum modules, and lower intermodular connectivity between default mode and frontoparietal modules than PD-N, correlated with Montreal Cognitive Assessment scores. Early-stage PD patients showed weaker small-worldization of brain networks. Modular connectivity alterations were mainly observed in patients with PD-M. These findings highlight the shared and distinct brain functional network dysfunctions in PD-M and PD-N, and yield insight into the neurobiology of cognitive decline in PD.

Key words: functional connectivity; graph theory; mild cognitive impairment; Parkinson's disease; psychoradiology; resting-state fMRI.

Introduction

Parkinson's disease (PD), as well as its hallmark motor symptoms, commonly causes a variable cognitive decline. Around 25–30% of PD individuals without dementia have mild cognitive impairment (PD-M), and 10–20% present as such at the time of diagnosis (Aarsland et al. 2017). Recognizing PD-M is clinically critical, as these individuals are more likely to progress to dementia: the conversion rate to dementia was 59% in patients with persistent PD-M at 1 year versus 7% in those with normal cognition during the first year (Pedersen et al. 2017). However, the neurobiology of PD-M is not fully understood.

Neuroimaging studies in PD find not only damage in specific brain regions, but also widespread disruptions of connections between different areas ("disconnection disorder") (Hall and Lewis 2019). These are conveniently defined using the brain connectome approach (Sporns et al. 2005), based on a graph theoretical analysis which characterizes complex systems by quantifying the topology of their network representations (Bullmore and Sporns 2009). This approach is particularly suitable for exploring cognition, which is not ascribable to individual brain regions, but rather arises from the whole-brain network organization and its interaction (Filippi et al. 2013).

Altered topological properties in both structural and functional networks are reported in PD-M (Baggio et al. 2014; Pereira et al. 2015; Galantucci et al. 2017; Mijalkov et al. 2017; Aracil-Bolanos et al. 2019). Functional network studies reveal increased global network segregation (Baggio et al. 2014) and nodal disruption centered on insular and inferior parietal regions (Aracil-Bolanos et al. 2019) in PD-M relative to PD-N, while structural network studies report decreased network integration and nodal disruption affecting mainly frontal and parietal regions

Received: November 1, 2021. **Revised:** December 18, 2021. **Accepted:** December 19, 2021

(Pereira et al. 2015; Galantucci et al. 2017). These studies are often inconsistent in detail. A key factor underlying these discrepancies is the clinical heterogeneity of participants: for example, dopaminergic medication can influence network metrics and mask the impact of PD on cognitive functions (Pereira et al. 2015); also some studies do not include healthy controls (HC), and thus lack a comparison with a reference network (Hassan et al. 2017; Lopes et al. 2017). Neurodegenerative diseases typically involve a cascade of pathophysiological alterations, so it is essential to investigate the early stages to minimize confounding factors. A technical issue is that functional networks capture the information transmission dynamics between areas more directly than do structural networks (Kelly et al. 2012).

To address these issues, this study uses graph theoretical analysis to compare the topology of brain functional networks in early-stage medication-free PD-M and PD-N individuals and a comparison group of HC. In the light of previous findings (Baggio et al. 2014; Pereira et al. 2015; Galantucci et al. 2017), we hypothesized that 1) there would be disruptions of network architecture, for example, decreased network integration and increased network segregation, in PD-M relative to PD-N and HC, and 2) these network abnormalities would be correlated with neuropsychological measures. Moreover, as PD-M is widely recognized as the translational state between normal cognitive functioning and dementia (Caviness et al. 2007; Litvan et al. 2012), and there is a progressive disruption of brain organization of functional network with the deterioration of cognitive dysfunction (Hassan et al. 2017; Lopes et al. 2017), we hypothesized that 3) there would be more widespread topological alterations in PD-M compared with PD-N.

Materials and Methods

Subjects

Individuals with PD were consecutively recruited from the movement disorders outpatient clinic of West China Hospital of Sichuan University between September 2013 and January 2016. We enrolled 24 PD-M individuals who met the Movement Disorder Society (MDS) Task Force criteria (Litvan et al. 2012) and 17 individuals with PD-N. We recruited 24 age- and sex-matched HC from the local area by poster advertisements. Exclusion criteria were prior learning disability, atypical Parkinsonian disorder, and history of other neurological conditions including vascular dementia, stroke, and moderate or severe head injury, major psychiatric or medical illness, as well as standard magnetic resonance imaging (MRI) exclusions. All patients were either drug-naïve ($N_{PD\text{-}N} = 8$, $N_{PD\text{-}M} = 12$) or scanned in an off state ($N_{PD\text{-}N} = 9$, $N_{PD\text{-}M} = 12$) defined as ≥12 h after the last dose of dopaminergic medication. Further details of exclusion criteria and evaluation are described in our previous studies (Suo et al. 2019; Suo, Lei, Li, Li, Kemp, et al. 2021; Suo, Lei, Li, Li, Peng, et al. 2021). Power analysis using G Power software (Faul et al. 2007) indicated that we needed a sample of at least 66 participants to detect a large-sized effect ($f = 0.4$, $\alpha = 0.05$, $1 - \beta = 0.8$) by one-way analysis of variance (ANOVA).

This study was approved by the local human research ethics committee, and written informed consent was obtained from all participants before enrollment. All procedures in this study conform to the ethical standards of the Declaration of Helsinki.

Clinical and Neuropsychological Assessments

Motor symptom severity was assessed using the MDS Unified PD Rating Scale part III (UPDRS-III) (Goetz et al. 2007) and Hoehn and Yahr (H&Y) stage (Goetz et al. 2004); diagnostic guidelines in China define those with H&Y stage ≤2.5 as early-stage PD (Chen et al. 2016). All participants underwent a comprehensive neuropsychological assessment of five cognitive domains (Litvan et al. 2012): attention/working memory: Trail Making Test Part A and Digit Span Backward task; executive function: category fluency test and 10 points Clock Drawing Test; language: Wechsler Adult Intelligence Scale-IV (WAIS-IV) and Similarities and Boston Naming Test; memory: Hopkins Verbal Learning Test (HVLT) and Brief Visuospatial Memory Test–Revised; visuospatial function: Clock Copying (CLOX-2) and Benton's Judgment of Line Orientation (JLO). Global cognitive screening was performed using the Montreal Cognitive Assessment (MoCA) (Dalrymple-Alford et al. 2010) and Mini Mental State Examination (MMSE). All neuropsychological evaluations were performed in the week before scanning. Mild cognitive impairment status in PD was assessed following the MDS Task Force level II criteria (Litvan et al. 2012), defined as test scores 1.5 standard deviation (SD) below the normative mean values for at least 2 neuropsychological tests within a domain or across different cognitive domains. PD-M patients were further divided into cognitive subtypes according to the Task Force criteria: single-domain subtype, with impairment on two tests within only one of the five cognitive domains; multiple-domain subtype, with impairment on at least one test across more than one cognitive domains (Cholerton et al. 2014).

Data Acquisition

MRI scanning was performed using a 3.0 T scanner (Tim Trio; Siemens Healthineers). Resting state functional MRI scanning parameters were as follows: repetition/echo time 2000/30 ms, flip angle 90°, matrix size 64 × 64, field of view 24 × 24 cm^2, voxel size 3.75 × 3.75 × 5 mm^3, slice thickness 5 mm without gap, 30 axial slices, and 240 volumes. Foam cushions were used to minimize head motion. All participants were instructed to be awake and relaxed with eyes closed. An experienced neuroradiologist evaluated and verified the quality of acquired images.

Data Preprocessing

Statistical Parametric Mapping (SPM12, http://www.fil.ion.ucl.ac.uk/spm) was used for data processing. The first 10 volumes were discarded to allow for magnetization equilibrium. After correction for intravolume

acquisition time delay and intervolume head motion, functional images were then spatially normalized to a standard template (Montreal Neurological Institute) and resampled into 3 mm isotropic voxels. None of the participants showed excessive head motion in terms of the criterion of translational movement >1.5 mm or rotation >1.5°. Next, the normalized data underwent temporal bandpass-filtering (0.01–0.08 Hz) and smoothing (full-width at half-maximum: 4 mm). The realigned images were regressed by Friston 24-parameter motion correction, and the global mean signal, white matter and cerebrospinal fluid signals were also regressed out. We used "head motion scrubbing" to minimize the impact of head movement (Power et al. 2014). Head motion measured by mean frame-wise displacement (FD) did not differ among the three groups (HC = 0.327 ± 0.142, PD-N = 0.238 ± 0.135, PD-M = 0.309 ± 0.183, $P = 0.192$, $F = 1.696$).

Network Construction

Functional connectivity networks were analyzed using the graph theoretical network analysis (GRETNA) toolbox (http://www.nitrc.org/projects/gretna/) (Wang et al. 2015). To define network nodes, we used automated anatomical labeling (AAL) atlas to parcel the brain into 116 regions of interest (ROIs) (Tzourio-Mazoyer et al. 2002). Pearson correlation coefficients of the mean time series between every pair of ROIs were calculated as network edges. This generated a weighted 116×116 correlation matrix for each participant.

In computing network metrics, a wide range of sparsity from 0.05 to 0.40 with steps of 0.01 was applied to the correlation matrices to ensure that the number of edges among the three groups were same (Zhang et al. 2011). Additionally, negative correlations were removed from all functional brain networks, given their ambiguous interpretation (Fox et al. 2009) and detrimental effects on test–retest reliability (Wang et al. 2011).

Network Metrics

The global and nodal metrics of each network were calculated at each sparsity threshold, after which the area under the curve (AUC) for each metric across the range of sparsity thresholds was computed (Zhang et al. 2011). The global metrics examined included clustering coefficient (C_p), normalized clustering coefficient (γ), characteristic path length (L_p), normalized characteristic path length (λ), and small worldness (σ) (Watts and Strogatz 1998), as well as the network efficiency including global efficiency (E_{glob}) and local efficiency (E_{loc}) (Latora and Marchiori 2001). Nodal metrics calculated for each node were nodal degree, nodal efficiency, and nodal betweenness (Achard and Bullmore 2007).

A modularity metric Q was also calculated to evaluate the degree to which the network is subdivided into specific modules, defined as subdivisions that have more intramodular than intermodular connections (Newman 2006). A modified greedy optimization algorithm (Danon et al. 2006) in GRETNA was applied to detect the optimal modular architecture by averaging all participants' functional networks. We then calculated the mean intra/within and inter-/between modular connectivity after applying the derived modular architecture.

Statistical Analysis

ANOVA was performed to compare the demographic and neuropsychological data between the three groups, and post hoc contrasts with Sidak correction. The qualitative variables were compared by the chi-square test. Clinical characteristics between PD-M and PD-N groups were analyzed using two-sample *t* tests.

Nonparametric permutation tests were performed to compare the AUC values of network metrics between the three groups, and post hoc analyses (10 000 permutations) (Ma et al. 2020). Statistical significance was set at $P < 0.05$. Partial correlations were used to explore the relationships of network metrics that showed significant group differences with neuropsychological variables in PD-M group, with age, sex, education years, illness duration, UPDRS III, and levodopa equivalent daily dose (LEDD) as covariates. Clinical diagnosis-by-sex/age interaction was analyzed using two-way ANOVA; if statistically significant interactions were observed, post hoc contrasts assessed the simple main effects.

Validation Analysis

Head Motion

We combined a series of strategies to minimize the effects of head motion, including removal of participants with excess gross head motion (>1.5 mm in translation or >1.5° in rotation), regression of 24-parameter head motion profiles (Yan et al. 2013), and scrubbing to censor "bad" volumes (FD > 0.5 mm) and volumes temporally close to the "bad" volumes (1 before and 2 after) for each participant before constructing individual functional networks (Power et al. 2012). We also performed statistical analysis on topological metrics with mean FD as a covariate.

Brain Parcellation

How best to define brain network nodes is the subject of ongoing research. Numerous brain parcellation methods are available and there is no agreed optimal choice for defining network nodes (Arslan et al. 2018). Choosing network nodes based on anatomic templates is popular, and so for this study we selected one of the most widely used AAL atlas. However, as recent studies suggest that this atlas cannot fully reflect functional organization of the brain (Eickhoff et al. 2018), we also reconstructed functional brain networks using a functionally defined atlas (Dosenbach et al. 2010); this includes 160 ROIs (5 mm radius spheres), identified from meta-analyses of task-related fMRI studies.

Results

Demographic and Neuropsychological Characteristics

Table 1 shows the demographic and neuropsychological characteristics of the participants. ANOVA revealed no significant differences in age, sex, or education years among the three groups. The two PD subgroups had no significant differences in the disease duration, mean age of onset, H&Y stage, LEDD, or UPDRS III (all $P < 0.05$).

Significant overall differences were observed among the three groups for MoCA and all the neuropsychological tests (all $P < 0.05$, Table 1) except MMSE, Digit Span Backward and CLOX-2 tests. In Sidak post hoc testing the PD-M group performed less well than the PD-N and HC groups on all the neuropsychological tests (all $P < 0.05$). In the PD-M group, there were four cases (17%) with single-domain impairment (2 executive, 1 attention, and 1 visuospatial domain) and 20 cases (83%) with multiple-domain impairment.

Global Topological Organization of Functional Brain Networks

The functional brain networks of the three groups exhibited larger $\gamma > 1$ and almost identical $\lambda \approx 1$ compared with those of random networks (Supplementary Fig. 1). Significant group effects were found in the AUCs of C_p, E_{loc}, E_{glob}, and L_p (Table 2, Fig. 1). Post hoc testing showed that relative to HC, both PD-M and PD-N had significantly lower C_p ($P = 0.007$ and 0.017), E_{loc} ($P = 0.007$ and 0.017), and E_{glob} ($P = 0.010$ and 0.010), and higher L_p ($P = 0.002$ and 0.005); there were no significant differences in global metrics between PD-M and PD-N.

Regional Topological Organization of Functional Brain Networks

Brain regions showing significant group differences in at least one nodal metric were identified. Significant group differences were revealed in bilateral Rolandic operculum (ROL), right Heschl gyrus, right superior temporal gyrus, left paracentral lobule, left supramarginal gyrus, right postcentral gyrus, and right fusiform gyrus ($P < 0.05$, FDR corrected). Post hoc testing showed that relative to HC, both PD subgroups had lower nodal efficiency and nodal degree in these regions (Table 2, Fig. 2). No significant differences in nodal metrics were observed between PD-M and PD-N.

Modular Architecture of Functional Brain Networks

Generated from all individuals, the detected modules included a sensorimotor module (I), default mode module (II), frontal–parietal module (III), subcortical module (IV), visual module (V), and cerebellum module (VI) (Fig. 3A, and Supplementary Material).

While modularity Q decreased as the cost of functional connectivity increased (Fig. 3B), there was no significant difference in the AUC between the three groups. Comparing "intramodular connectivity" among the three groups revealed significant group differences for sensorimotor, default mode, subcortical, and cerebellum modules ($P < 0.05$, FDR corrected). Post hoc testing revealed that relative to HC, the PD-M group had significantly decreased intramodular connectivity for sensorimotor, default mode, subcortical, and cerebellum modules; compared with HC, PD-N had significantly decreased intramodular connectivity for the sensorimotor module; compared with PD-N, PD-M had significantly decreased intramodular connectivity for the default mode, subcortical and cerebellum modules (Fig. 3C). Comparing intermodular connectivity among the three groups, there were significant group differences in intermodular connectivity for sensorimotor and visual modules, default mode and frontal–parietal modules, and default mode and visual modules ($P < 0.05$, FDR corrected). Post hoc testing revealed that relative to HC, PD-M showed significantly decreased intermodular connectivity for sensorimotor and visual modules, default mode, and frontal–parietal modules, and default mode and visual modules; compared with HC, there were no statistically significant PD-N specific intermodular connectivity alterations; relative to PD-N, PD-M had significantly decreased intermodular connectivity for the default mode and frontoparietal modules (Fig. 3D). No significant differences were found among the three groups in intermodular connectivity for other pairs of modules.

Relationships between Network Metrics and Neuropsychological Data

As shown in Figure 4, in the PD-M group, MoCA scores were positively correlated with intramodular connectivity of default mode module (II) ($r = 0.510$, $P = 0.031$) and cerebellum module (VI) ($r = 0.500$, $P = 0.035$), and intermodular connectivity between default mode module (II) and frontal–parietal module (III) ($r = 0.488$, $P = 0.040$); WAIS-IV Similarities scores were positively correlated with E_{glob} ($r = 0.493$, $P = 0.037$) and the nodal efficiency of right ROL ($r = 0.582$, $P = 0.011$), and negatively correlated with L_p ($r = -0.521$, $P = 0.027$). However, these correlations did not survive multiple comparison corrections at FDR corrected <0.05. There were no significant relationships between other measures and cognitive scores ($P > 0.05$).

Interaction between Groups and Sex/Age with Respect to Network Metrics

Two-way ANOVA revealed no significant diagnosis-by-sex interaction or diagnosis-by-age interaction in any of the network metrics that showed significant group differences (all $P > 0.05$, Supplementary Table 1).

Reproducibility/Validity

The main results of functional networks were largely reproducible when different strategies were used to control head motion (Supplementary Table 2), and to define network nodes (Supplementary Table 3).

Table 1. Characteristics of participants

	Groups			ANOVA	Effect size η^2/Cohen's d/C	Confidence interval	Power	Group comparisons P*		
	HC	PD-N	PD-M	p				HC vs. PD-N	HC vs. PD-M	PD-N vs. PD-M
Demographic characteristics										
Number	24	17	24							
Age (years)	55.4 ± 6.5	54.0 ± 8.2	54.3 ± 8.3	0.808	0.007	0, 0.044	0.084	0.916	0.936	0.999
Sex (male/female)#	11/13 (46/54%)	10/7 (59/41%)	9/15 (38/62%)	0.402	0.165	0, 0.379	0.392	0.412	0.558	0.177
Years of education	10.3 ± 3.3	11.4 ± 2.5	9.6 ± 3.4	0.233	0.049	0, 0.142	0.340	0.640	0.893	0.246
Clinical characteristics										
Age at onset (years)	—	50.9 ± 8.9	51.0 ± 9.0	—	−0.002	−0.623, 0.619	0.050	—	—	0.995¶
Disease duration (years)	—	2.2 ± 1.6	3.3 ± 2.8	—	−0.439	−1.103, 0.231	0.272	—	—	0.200¶
H&Y stage	—	1.8 ± 0.6	1.9 ± 0.6	—	−0.137	−0.758, 0.486	0.071	—	—	0.669¶
LEDD (mg/day)	—	241 ± 305	291 ± 356	—	−0.149	−0.771, 0.474	0.074	—	—	0.640¶
UPDRS III	—	17.1 ± 9.7	24.3 ± 12.5	—	−0.630	−1.263, 0.011	0.491	—	—	0.054¶
Global cognitive function										
MMSE	28.0 ± 1.7	28.8 ± 1.0	27.7 ± 2.0	0.135	0.064	0, 0.162	0.437	0.339	0.944	0.146
MoCA	22.9 ± 3.2	24.3 ± 2.4	19.3 ± 2.9	**<0.001**	0.361	0.192, 0.476	0.999	0.328	**<0.001**	**<0.001**
Attention and working memory										
TMT-A	52.5 ± 22.1	49.2 ± 11.0	71.3 ± 45.6	**0.048**	0.094	0.001, 0.202	0.615	0.740	**0.041**	**0.029**
Digit span Backward	4.4 ± 1.4	5.0 ± 1.3	4.3 ± 1.2	0.216	0.051	0, 0.143	0.353	0.456	0.979	0.250
Executive function										
Category fluency test	19.3 ± 5.8	19.7 ± 3.9	15.9 ± 4.6	**0.022**	0.122	0.010, 0.239	0.751	0.994	0.061	**0.047**
CDT	12.4 ± 1.3	12.5 ± 1.8	10.5 ± 3.3	**0.010**	0.153	0.023, 0.277	0.859	0.999	**0.031**	**0.026**
Language										
WAIS-IV Similarities	14.6 ± 4.0	15.9 ± 3.4	12.3 ± 3.7	**0.012**	0.147	0.019, 0.272	0.841	0.681	0.175	**0.012**
BNT	24.2 ± 2.8	26.0 ± 1.5	22.7 ± 3.6	**0.003**	0.191	0.044, 0.319	0.938	0.222	0.273	**0.002**
Memory										
HVLT	20.7 ± 5.3	22.3 ± 3.6	15.6 ± 4.3	**<0.001**	0.339	0.153, 0.465	0.999	0.688	**0.004**	**<0.001**
BVMT-R	20.6 ± 6.0	22.6 ± 3.6	16.8 ± 5.9	**0.004**	0.192	0.042, 0.322	0.940	0.651	0.099	**0.003**
Visuospatial function										
JLO	19.9 ± 3.3	23.3 ± 3.6	17.2 ± 6.0	**0.001**	0.239	0.074, 0.370	0.983	0.144	0.226	**<0.001**
CLOX-2	14.1 ± 1.2	14.1 ± 1.0	13.5 ± 1.1	0.161	0.059	0, 0.156	0.405	0.999	0.263	0.301

Data presented as mean ± standard deviation unless otherwise indicated. *P-values by post hoc Sidak correction for three comparisons unless otherwise indicated. #P-values by χ^2 test. ¶P-values by using two-sample t tests. Abbreviations: ANOVA, analysis of variance; BNT, Boston Naming Test; BVMT-R, Brief Visuospatial Memory Test-Revised; CDT, Clock Drawing Test; CLOX-2, Clock Copying; HC, healthy controls; HVLT, Hopkins Verbal Learning Test; H&Y stage, Hoehn and Yahr stage; JLO, Benton's Judgment of Line Orientation; LEDD, Levodopa equivalent daily dose; MMSE, Mini–Mental State Examination; MoCA, Montreal Cognitive Assessment; PD, Parkinson's disease; PD-M, PD with mild cognitive impairment; PD-N, PD with normal cognition; TMT-A, Trail Making Test Part A; UPDRS, Unified PD Rating Scale; WAIS, Wechsler Adult Intelligence Scale.

Table 2. Brain topological metrics showing significant differences between the groups

	Groups			P (F)	Effect size η^2	Confidence intervals	Power	Group comparisons P (t)		
Measurements	HC	PD-N	PD-M					HC vs. PD-N	HC vs. PD-M	PD-N vs. PD-M
Global										
Global efficiency	0.085 ± 0.007	0.080 ± 0.006	0.079 ± 0.009	**0.028** (3.579)	0.104	0.004, 0.214	0.668	**0.010** (2.123)	**0.010** (2.366)	0.341 (0.432)
Local efficiency	0.133 ± 0.018	0.123 ± 0.011	0.120 ± 0.019	**0.026** (3.629)	0.105	0.005, 0.216	0.673	**0.017** (1.965)	**0.007** (2.364)	0.284 (0.579)
Clustering coefficient	0.101 ± 0.018	0.091 ± 0.011	0.088 ± 0.018	**0.029** (3.665)	0.106	0.005, 0.217	0.678	**0.017** (2.011)	**0.007** (2.381)	0.320 (0.479)
Characteristic path length	1.473 ± 0.100	1.549 ± 0.095	1.577 ± 0.143	**0.009** (5.033)	0.140	0.021, 0.257	0.819	**0.005** (−2.430)	**0.002** (−2.926)	0.241 (−0.715)
Nodal efficiency										
L Rolandic operculum	0.095 ± 0.009	0.087 ± 0.008	0.084 ± 0.008	<**0.001** (11.847)	0.277	0.116, 0.398	0.995	**0.001** (3.004)	<**0.001** (4.728)	0.092 (1.358)
R Rolandic operculum	0.095 ± 0.008	0.087 ± 0.009	0.085 ± 0.010	**0.001** (8.305)	0.211	0.065, 0.334	0.962	**0.001** (3.116)	<**0.001** (3.854)	0.258 (0.642)
L supramarginal gyrus	0.088 ± 0.010	0.079 ± 0.007	0.077 ± 0.008	<**0.001** (10.936)	0.261	0.103, 0.383	0.991	**0.001** (3.160)	<**0.001** (4.165)	0.202 (0.832)
R superior temporal gyrus	0.092 ± 0.009	0.084 ± 0.010	0.081 ± 0.010	<**0.001** (8.082)	0.207	0.062, 0.329	0.958	**0.006** (2.510)	<**0.001** (3.981)	0.149 (1.059)
R Heschl gyrus	0.090 ± 0.011	0.081 ± 0.010	0.078 ± 0.012	**0.001** (7.174)	0.188	0.050, 0.310	0.934	**0.004** (2.735)	**0.001** (3.514)	0.240 (0.729)
L paracentral lobule	0.082 ± 0.012	0.072 ± 0.007	0.069 ± 0.010	<**0.001** (10.961)	0.261	0.103, 0.384	0.991	**0.001** (3.124)	<**0.001** (4.155)	0.139 (1.089)
R postcentral gyrus	0.090 ± 0.009	0.079 ± 0.011	0.079 ± 0.010	<**0.001** (9.736)	0.239	0.086, 0.362	0.983	**0.001** (3.549)	<**0.001** (4.159)	0.447 (0.129)
R fusiform gyrus	0.095 ± 0.010	0.084 ± 0.007	0.085 ± 0.013	**0.001** (6.807)	0.180	0.044, 0.301	0.920	<**0.001** (3.978)	**0.003** (2.807)	0.384 (−0.369)
Nodal degree										
L Rolandic operculum	5.026 ± 0.930	4.259 ± 1.054	3.904 ± 0.921	<**0.001** (8.488)	0.215	0.068, 0.338	0.966	**0.009** (2.463)	<**0.001** (4.203)	0.138 (1.146)
L paracentral lobule	3.576 ± 1.350	2.671 ± 0.878	2.269 ± 0.573	<**0.001** (10.691)	0.256	0.099, 0.379	0.990	**0.009** (2.421)	<**0.001** (4.369)	0.044 (1.777)
R postcentral gyrus	4.619 ± 1.157	3.424 ± 1.340	3.361 ± 1.127	**0.001** (8.043)	0.206	0.062, 0.329	0.957	**0.002** (3.052)	<**0.001** (3.817)	0.441 (0.163)
R Heschl gyrus	4.401 ± 1.202	3.492 ± 0.985	3.219 ± 1.066	**0.001** (7.459)	0.194	0.053, 0.316	0.943	**0.008** (2.563)	**0.001** (3.603)	0.198 (0.833)
R fusiform gyrus	5.339 ± 1.036	4.101 ± 0.928	4.187 ± 1.408	**0.001** (7.904)	0.203	0.060, 0.326	0.954	<**0.001** (3.932)	**0.001** (3.229)	0.421 (−0.221)
R superior temporal gyrus	4.646 ± 1.111	3.896 ± 1.038	3.614 ± 0.839	**0.002** (6.757)	0.179	0.044, 0.300	0.918	**0.016** (2.187)	<**0.001** (3.633)	0.177 (0.962)

Metrics shown as mean ± standard deviation. Comparisons of the area under the curve of global and nodal metrics among the three groups and post hoc pairwise comparisons were performed using nonparametric permutation tests. For the nodal metrics, the false discovery rate was calculated using multiple comparison correction. There were no significant differences in nodal betweenness. For the post hoc tests, $P < 0.05/3$ was considered significant (shown in **bold**). Abbreviations: PD, Parkinson's disease; PD-M, PD with mild cognitive impairment; PD-N, PD with normal cognition; HC, healthy controls; L, left; R, right.

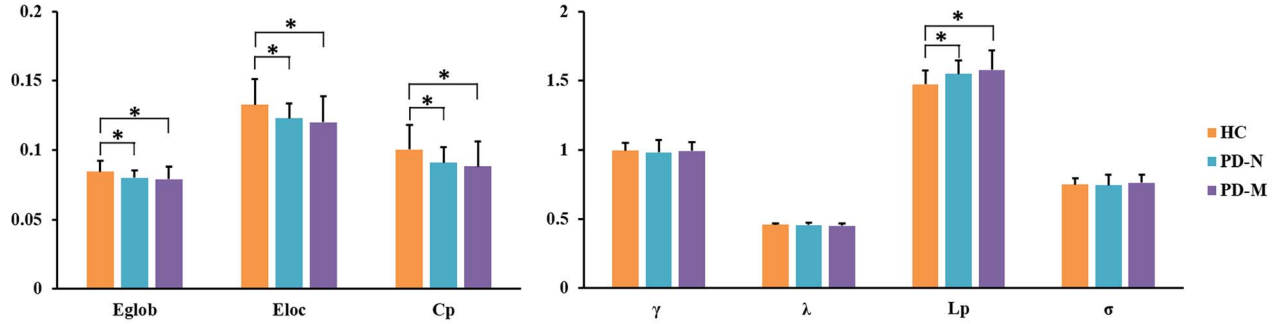

Figure 1. Global network properties in the three groups. The y-axis is the area under the curve of each of the global network parameters (identified on the x-axis) and the three groups are color coded as in the key. Error bars denote standard deviation. Asterisks indicate significant differences ($P < 0.05$) in post hoc testing. Abbreviations: PD, Parkinson's disease; PD-M, PD with mild cognitive impairment; PD-N, PD with normal cognition; HC, healthy control. Network parameters: Cp, clustering coefficient; γ, normalized clustering coefficient; Lp, characteristic path length; λ, normalized characteristic path length; Eloc, local efficiency; Eglob, global efficiency; σ, small worldness.

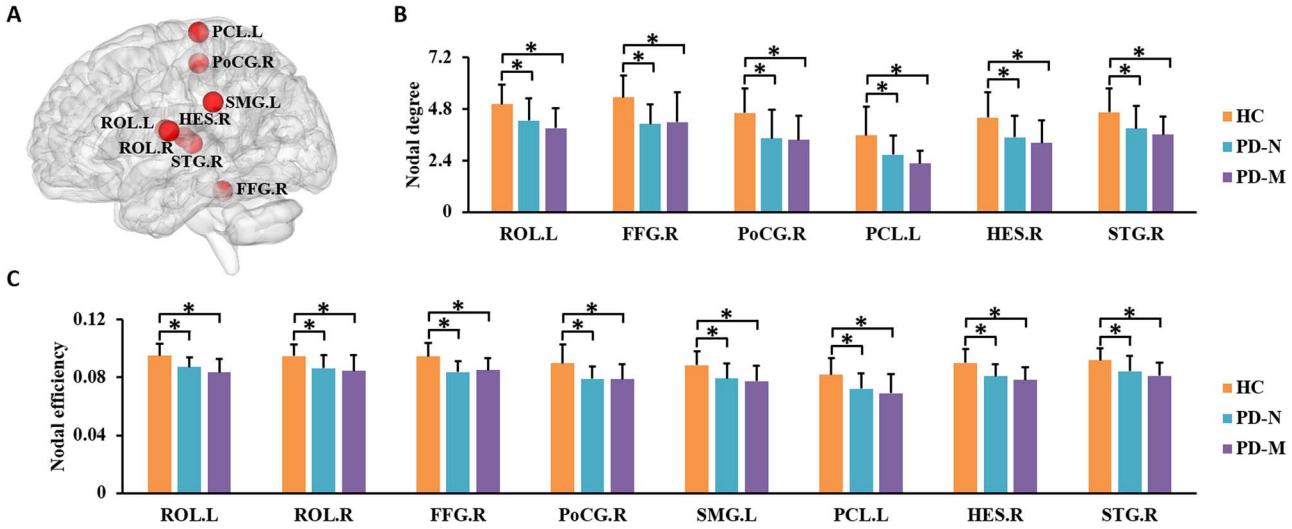

Figure 2. Brain regions showing abnormal nodal centrality in functional brain networks in the three groups. In (A), regions with significant group differences ($P < 0.05$, FDR corrected) are visualized using the BrainNet viewer (http://www.nitrc.org/projects/bnv). The bar graphs show the post hoc pairwise comparisons with significant differences in (B) nodal degree and (C) nodal efficiency. The y-axes are the area under the curve of the two network parameters and the three groups are color coded as in the key. The x-axis shows the brain regions. Abbreviations: PD, Parkinson's disease; PD-M, PD with mild cognitive impairment; PD-N, PD with normal cognition; HC, healthy control; ROL, Rolandic operculum; FFG, fusiform gyrus; PoCG, postcentral gyrus; SMG, supramarginal gyrus; PCL, paracentral lobule; HES, Heschl gyrus; STG, superior temporal gyrus; L, left; R, right.

Discussion

By investigating early-stage medication-free PD-M individuals and demographically matched PD-N and HC, we found global, nodal, and modular functional network alterations relative to HC across the two PD subgroups, generally more abnormal in PD-M than PD-N. At the global level, we observed lower C_p, E_{loc}, and E_{glob}, and higher L_p in PD-M and PD-N relative to HC; L_p and E_{glob} were correlated with language domain scores in PD-M. At the regional level, both PD subgroups had lower nodal metrics in sensorimotor regions than HC. At the modular level, the PD-M group had, compared with PD-N, lower intramodular connectivity in default mode, subcortical and cerebellum modules, and lower intermodular connectivity between default mode and frontoparietal modules, correlated with MoCA scores.

At the global level, network analysis of this kind characterizes both integration (reflected by L_p, E_{glob}, and λ) and segregation (reflected by C_p, E_{loc}, and γ) of neural information (Suo et al. 2018). Compared with HC, individuals with PD had decreased network segregation (lower C_p and E_{loc}) and decreased network integration (lower E_{glob} and higher L_p), representing a shift toward "weaker small-worldization" (Suo et al. 2018), possibly as a result of neurodegeneration. These observations are largely compatible with previous brain network studies in PD (Pereira et al. 2015; Galantucci et al. 2017; Suo et al. 2017; Sreenivasan et al. 2019). Apparently at variance with this, one functional connectome study reported increased network segregation (higher C_p) in PD-M with no significant change in network integration (Baggio et al. 2014); however, that was in medicated individuals in the on-state, and medication can affect network measures (Achard and Bullmore 2007; Lopes et al. 2017). The correlation between altered L_p and E_{glob} and language cognitive domain scores in PD-M is compatible with, but of course does not prove, a causal role for

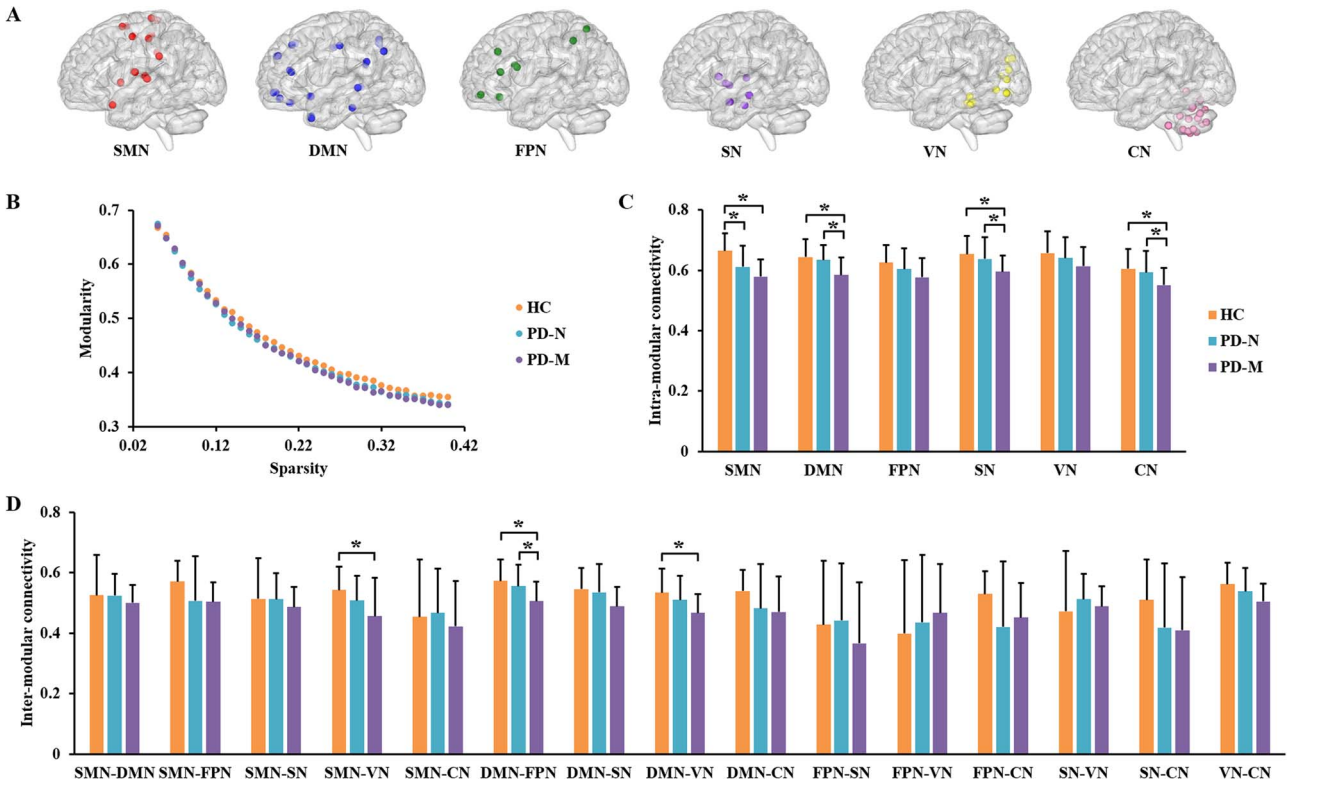

Figure 3. Modular characteristics of functional brain networks in the three groups. (*A*) Six modules which were identified using combined data from all three groups: Details are given in supplementary materials. (*B*) Network modularity (*Q*) as a function of sparsity: Modularity Q monotonically decreased as a function of increasing cost, the AUC of which did not differ among the three groups. The bar graphs show data with post hoc pairwise comparisons showing significant between-group differences in (*C*) intramodular and (*D*) intermodular connectivity. Abbreviations: PD, Parkinson's disease; PD-M, PD with mild cognitive impairment; PD-N, PD with normal cognition; HC, healthy controls; SMN, sensorimotor network; DMN, default mode network; FPN, frontal–parietal network; SN, subcortical network; VN, visual network; CN, cerebellum network.

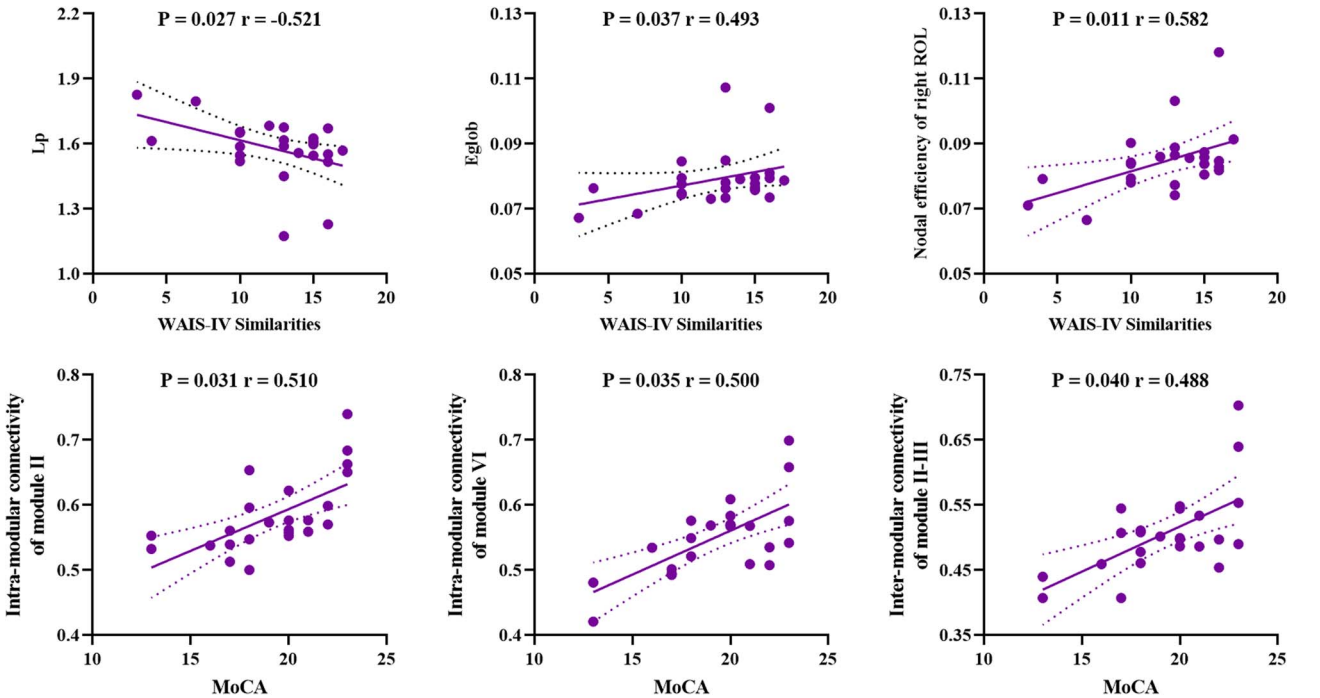

Figure 4. The relationships between network measures and clinical variables in Parkinson's disease with mild cognitive impairment. Abbreviations: Lp, characteristic path length; Eglob, global efficiency; WAIS, Wechsler adult intelligence scale; ROL, Rolandic operculum; MoCA, Montreal cognitive assessment; module II, default mode network; module III, frontal-parietal network; module VI, cerebellum network.

disrupted global network integration in the development of specific cognitive impairments.

At the regional level, both PD subgroups had abnormal nodal metrics in sensorimotor regions; most of these regions have been reported to show other abnormalities in nondemented PD, such as functional disconnection (Agosta et al. 2017; Tuovinen et al. 2018), hypometabolism (Hu et al. 2000), and cortical atrophy (Xu et al. 2018). These regions also overlap with locations where cortical Lewy neurites and Lewy bodies are found in symptomatic PD, corresponding to Braak's stages 4 and 5 (Braak et al. 2003). Nodal efficiency of right ROL, one of the major regions involved in language processing (Indefrey et al. 2001), was positively correlated with language domain (WAIS-IV similarities) scores, again at least compatible with a causal role in cognitive impairment.

At the modular level, PD-M had widespread alterations compared with HC, while PD-N had very few. On direct comparison, we found distinct decreases of intramodular connectivity in the default mode, subcortical and cerebellum modules in PD-M relative to PD-N. We also found significant correlations of modular properties with global cognitive function (as measured by MoCA scores). These modular abnormalities make some pathophysiological sense. Disruption of the default mode network is related to cognitive deficits in PD (Baggio et al. 2015), and its functional integrity in PD-M has recently been related to reversion to cognitively normal status (Chung et al. 2019). These and our findings all implicate functional disruption of the default mode network as part of the neural substrate of PD-M. Cognitive abnormalities, especially executive dysfunction, are assumed to be caused by dopaminergic depletion involving subcortical circuits (Kudlicka et al. 2011; Pan et al. 2021). This may underlie the decreased intraconnectivity we observed in the subcortical module. The cerebellum takes part in both sensorimotor and cognitive processing (Kansal et al. 2017; Lan et al. 2021; Suo, Lei, Li, Li, Dai, et al. 2021). Our finding of decreased intraconnectivity in the cerebellar module, consistent with a recent functional study showing cerebellar alterations in PD-M (Li et al. 2021), suggests that cerebellum may play a role in the pathogenesis of PD-M. Moreover, cognitive impairment can contribute to movement disorders (e.g., gait) in some individuals with PD (Avanzino et al. 2018). This could be related to our finding of lower intermodular connectivity between visual and sensorimotor modules. These results support the view that cognitive deficits in PD-M are the consequence of modular level disruption of complex brain functional networks.

Direct comparison revealed no significant difference between the two PD subgroups at the global and nodal levels. It may be that these differences are too subtle to detect given our relatively small sample size, and the fact that our patients were at the newly diagnosed early stage with mean disease duration of 1.8 years, which may give limited scope for topologic metrics to diverge between the two PD subgroups. Although small-world organization at global and nodal levels describes the key topological properties of complex networks, it does not provide information about the intermediate scale organization, which is more completely described by the modular architecture (Meunier et al. 2010). As disruption of modules is known to be closely associated with cognitive impairment (de Haan et al. 2012; Wang et al. 2013), it is not surprising that our PD subgroups differed significantly in modular characteristics.

It is notable that a generally consistent pattern (increasing or decreasing) is observed across the three groups (e.g., Figures 1 and 2). This is consistent with a recent graph theory study finding increasing disruption of topographic organization as cognitive impairment worsens in PD (Hou et al. 2020), and earlier reports of more severe disruption of network organization in cognitively impaired compared with cognitively preserved patients (Pereira et al. 2015; Hassan et al. 2017; Lopes et al. 2017). Altogether, the network metrics support the idea of progressive decline from PD-N to PD-M, although of course a longitudinal study would be required to prove that.

Our study has several limitations. First, while it provides information about network topology, the detection of group differences may have been limited by the relatively small sample size resulting from our strict recruitment criteria. However, findings of several network studies using the Parkinson's Progression Markers Initiative database (PPMI) (https://www.ppmi-info.org/) (Pereira et al. 2015; Mijalkov et al. 2017; Sreenivasan et al. 2019) are mostly in line with our results. Although representative of early stages of PD, both our sample and the PPMI database are research-based cohorts which may not be fully representative of a community-based sample. To develop a comprehensive model of baseline topological network dysfunction will require larger PD samples adhering to stringent criteria to maintain a sufficiently homogenous group of subjects, while still respecting the inherent heterogeneity of the disease. Second, it was a cross-sectional design. Longitudinal studies would give more direct information about functional network progression from PD-N to PD-M. Third, although medications were withdrawn prior to MRI scanning, the potential confounding effects of chronic dopaminergic medications cannot be completely eliminated. Fourth, applying a more stringent cut-off score (e.g., <2 SDs below normative data) may reduce the risk of Type 1 errors in research and clinical settings (Goldman et al. 2013). In keeping with previous studies, impairment on a neuropsychological test was defined as a score at least 1.5 SDs below normative means in this study, which was considered the best trade-off between type I and II errors (Liepelt-Scarfone et al. 2011). Fifth, the optimal strategy for node definition is still lacking. The AAL atlas was used to divide the brain into 116 ROIs in our study, and the functionally defined Dosenbach atlas (160 ROIs) were used for reproducibility/validation analyses. However, available connectome studies are restricted to the

macroscopic scale and do not provide information on the functionally important microscopic dimension (Amunts et al. 2013). It would be interesting to explore underlying patterns further by combining microscopic scale techniques from the perspective of complex networks. Future studies using different parcellation strategies will provide more comprehensive insights. Finally, the correlations between network measures and neuropsychological tests did not survive multiple comparison corrections, and should therefore be considered exploratory.

In conclusion, our findings provide evidence for shared and distinct patterns of functional network disruptions between PD-M and PD-N at global, nodal, and modular levels. Most of the network measures have a common trend, such that PD-M showed more abnormal values than PD-N. Only PD-M had significantly widespread alterations, especially at the modular level involving multiple networks including default mode, subcortical and cerebellar regions. Specifically, this study adds to the field of psychoradiology (Sun et al. 2015; Lui et al. 2016; Gong 2020; Li et al. 2021; Suo et al. 2022), an evolving subspecialty of radiology, which is primed to be of major clinical importance in guiding diagnostic and therapeutic decision making in patients with neuropsychiatric disorders.

Supplementary Material

Supplementary material can be found at *Cerebral Cortex* online.

Data Availability

The data that support the findings of present study are available from the corresponding author through reasonable request.

Authors' Contributions

Q.G. and R.P. conceived the idea for the study and managed the project. X.S., D.L., and N.L. designed the study. X.S., D.L., N.L, J.P., and C.C. collected the data. X.S., W.L., and K.Q. performed the data analyses. X.S. drafted the main article. G.J.K. critically reviewed the manuscript. All authors approved for publication.

Funding

National Natural Science Foundation of China (grants 81621003, 81820108018, 82001800, 82027808); China Postdoctoral Science Foundation (grant 2020 M683317); Science and Technology Support Program of Sichuan Province (grant 22MZGC0308); Science and Technology Project of Chengdu City (grant 2021-YF05-01587-SN); Post-Doctor Research Project, West China Hospital, Sichuan University (grant 2019HXBH104).

Notes

Conflict of Interest: The authors have declared that no conflict of interest exists.

References

Aarsland D, Creese B, Politis M, Chaudhuri KR, Ffytche DH, Weintraub D, Ballard C. 2017. Cognitive decline in Parkinson disease. *Nat Rev Neurol*. 13:217–231.

Achard S, Bullmore E. 2007. Efficiency and cost of economical brain functional networks. *PLoS Comput Biol*. 3:e17.

Agosta F, Gatti R, Sarasso E, Volonte MA, Canu E, Meani A, Sarro L, Copetti M, Cattrysse E, Kerckhofs E, et al. 2017. Brain plasticity in Parkinson's disease with freezing of gait induced by action observation training. *J Neurol*. 264:88–101.

Amunts K, Lepage C, Borgeat L, Mohlberg H, Dickscheid T, Rousseau ME, Bludau S, Bazin PL, Lewis LB, Oros-Peusquens AM, et al. 2013. BigBrain: an ultrahigh-resolution 3D human brain model. *Science*. 340:1472–1475.

Aracil-Bolanos I, Sampedro F, Marin-Lahoz J, Horta-Barba A, Martinez-Horta S, Boti M, Perez-Perez J, Bejr-Kasem H, Pascual-Sedano B, Campolongo A, et al. 2019. A divergent breakdown of neurocognitive networks in Parkinson's disease mild cognitive impairment. *Hum Brain Mapp*. 40:3233–3242.

Arslan S, Ktena SI, Makropoulos A, Robinson EC, Rueckert D, Parisot S. 2018. Human brain mapping: a systematic comparison of parcellation methods for the human cerebral cortex. *NeuroImage*. 170:5–30.

Avanzino L, Lagravinese G, Abbruzzese G, Pelosin E. 2018. Relationships between gait and emotion in Parkinson's disease: a narrative review. *Gait Posture*. 65:57–64.

Baggio HC, Sala-Llonch R, Segura B, Marti MJ, Valldeoriola F, Compta Y, Tolosa E, Junque C. 2014. Functional brain networks and cognitive deficits in Parkinson's disease. *Hum Brain Mapp*. 35:4620–4634.

Baggio HC, Segura B, Sala-Llonch R, Marti MJ, Valldeoriola F, Compta Y, Tolosa E, Junque C. 2015. Cognitive impairment and resting-state network connectivity in Parkinson's disease. *Hum Brain Mapp*. 36:199–212.

Braak H, Del Tredici K, Rub U, de Vos RA, Jansen Steur EN, Braak E. 2003. Staging of brain pathology related to sporadic Parkinson's disease. *Neurobiol Aging*. 24:197–211.

Bullmore E, Sporns O. 2009. Complex brain networks: graph theoretical analysis of structural and functional systems. *Nat Rev Neurosci*. 10:186–198.

Caviness JN, Driver-Dunckley E, Connor DJ, Sabbagh MN, Hentz JG, Noble B, Evidente VG, Shill HA, Adler CH. 2007. Defining mild cognitive impairment in Parkinson's disease. *Mov Disord*. 22:1272–1277.

Chen S, Chan P, Sun S, Chen H, Zhang B, Le W, Liu C, Peng G, Tang B, Wang L, et al. 2016. The recommendations of Chinese Parkinson's disease and movement disorder society consensus on therapeutic management of Parkinson's disease. *Transl Neurodegener*. 5:12.

Cholerton BA, Zabetian CP, Wan JY, Montine TJ, Quinn JF, Mata IF, Chung KA, Peterson A, Espay AJ, Revilla FJ, et al. 2014. Evaluation of mild cognitive impairment subtypes in Parkinson's disease. *Mov Disord*. 29:756–764.

Chung SJ, Park YH, Yoo HS, Lee YH, Ye BS, Sohn YH, Lee JM, Lee PH. 2019. Mild cognitive impairment reverters have a favorable cognitive prognosis and cortical integrity in Parkinson's disease. *Neurobiol Aging*. 78:168–177.

Dalrymple-Alford JC, MacAskill MR, Nakas CT, Livingston L, Graham C, Crucian GP, Melzer TR, Kirwan J, Keenan R, Wells S, et al. 2010. The MoCA: well-suited screen for cognitive impairment in Parkinson disease. *Neurology*. 75:1717–1725.

Danon L, Díaz-Guilera A, Arenas A. 2006. The effect of size heterogeneity on community identification in complex networks. *J Stat Mech: Theory Exp*. 2006:P11010.

de Haan W, van der Flier WM, Koene T, Smits LL, Scheltens P, Stam CJ. 2012. Disrupted modular brain dynamics reflect cognitive dysfunction in Alzheimer's disease. *NeuroImage*. 59:3085–3093.

Dosenbach NUF, Nardos B, Cohen AL, Fair DA, Power JD, Church JA, Nelson SM, Wig GS, Vogel AC, Lessov-Schlaggar CN, et al. 2010. Prediction of individual brain maturity using fMRI. *Science*. 329: 1358–1361.

Eickhoff SB, Constable RT, Yeo BTT. 2018. Topographic organization of the cerebral cortex and brain cartography. *NeuroImage*. 170: 332–347.

Faul F, Erdfelder E, Lang A-G, Buchner A. 2007. G*Power 3: a flexible statistical power analysis program for the social, behavioral, and biomedical sciences. *Behav Res Methods*. 39:175–191.

Filippi M, van den Heuvel MP, Fornito A, He Y, Hulshoff Pol HE, Agosta F, Comi G, Rocca MA. 2013. Assessment of system dysfunction in the brain through MRI-based connectomics. *Lancet Neurol*. 12: 1189–1199.

Fox MD, Zhang D, Snyder AZ, Raichle ME. 2009. The global signal and observed anticorrelated resting state brain networks. *J Neurophysiol*. 101:3270–3283.

Galantucci S, Agosta F, Stefanova E, Basaia S, van den Heuvel MP, Stojkovic T, Canu E, Stankovic I, Spica V, Copetti M, et al. 2017. Structural brain connectome and cognitive impairment in Parkinson disease. *Radiology*. 283:515–525.

Goetz CG, Poewe W, Rascol O, Sampaio C, Stebbins GT, Counsell C, Giladi N, Holloway RG, Moore CG, Wenning GK, et al. 2004. Movement disorder society task force report on the Hoehn and Yahr staging scale: status and recommendations. *Mov Disord*. 19: 1020–1028.

Goetz CG, Fahn S, Martinez-Martin P, Poewe W, Sampaio C, Stebbins GT, Stern MB, Tilley BC, Dodel R, Dubois B, et al. 2007. Movement disorder society-sponsored revision of the unified Parkinson's disease rating scale (MDS-UPDRS): process, format, and clinimetric testing plan. *Mov Disord*. 22:41–47.

Goldman JG, Holden S, Bernard B, Ouyang BC, Goetz CG, Stebbins GT. 2013. Defining optimal cutoff scores for cognitive impairment using movement disorder society task force criteria for mild cognitive impairment in Parkinson's disease. *Mov Disord*. 28: 1972–1979.

Gong Q. 2020. *Psychoradiology*, Vol. 30. New York: Elsevier Inc. Neuroimaging Clinics of North America, pp. 1–123.

Hall JM, Lewis SJG. 2019. Neural correlates of cognitive impairment in Parkinson's disease: a review of structural MRI findings. *Int Rev Neurobiol*. 144:1–28.

Hassan M, Chaton L, Benquet P, Delval A, Leroy C, Plomhause L, Moonen AJ, Duits AA, Leentjens AF, van Kranen-Mastenbroek V, et al. 2017. Functional connectivity disruptions correlate with cognitive phenotypes in Parkinson's disease. *Neuroimage Clin*. 14: 591–601.

Hou Y, Wei Q, Ou R, Yang J, Gong Q, Shang H. 2020. Impaired topographic organization in Parkinson's disease with mild cognitive impairment. *J Neurol Sci*. 414:116861.

Hu MT, Taylor-Robinson SD, Chaudhuri KR, Bell JD, Labbe C, Cunningham VJ, Koepp MJ, Hammers A, Morris RG, Turjanski N, et al. 2000. Cortical dysfunction in non-demented Parkinson's disease patients: a combined (31)P-MRS and (18)FDG-PET study. *Brain*. 123(Pt 2):340–352.

Indefrey P, Brown CM, Hellwig F, Amunts K, Herzog H, Seitz RJ, Hagoort P. 2001. A neural correlate of syntactic encoding during speech production. *Proc Natl Acad Sci U S A*. 98:5933–5936.

Kansal K, Yang Z, Fishman AM, Sair HI, Ying SH, Jedynak BM, Prince JL, Onyike CU. 2017. Structural cerebellar correlates of cognitive and motor dysfunctions in cerebellar degeneration. *Brain*. 140: 707–720.

Kelly C, Biswal BB, Craddock RC, Castellanos FX, Milham MP. 2012. Characterizing variation in the functional connectome: promise and pitfalls. *Trends Cogn Sci*. 16:181–188.

Kudlicka A, Clare L, Hindle JV. 2011. Executive functions in Parkinson's disease: systematic review and meta-analysis. *Mov Disord*. 26:2305–2315.

Lan H, Suo X, Li W, Li N, Li J, Peng J, Lei D, Sweeney JA, Kemp GJ, Peng R, et al. 2021. Abnormalities of intrinsic brain activity in essential tremor: a meta-analysis of resting-state functional imaging. *Hum Brain Mapp*. 42:3156–3167.

Latora V, Marchiori M. 2001. Efficient behavior of small-world networks. *Phys Rev Lett*. 87:198701.

Li F, Sun H, Biswal BB, Sweeney JA, Gong Q. 2021. Artificial intelligence applications in psychoradiology. *Psychoradiology*. 1:94–107.

Li MG, Bian XB, Zhang J, Wang ZF, Ma L. 2021. Aberrant voxel-based degree centrality in Parkinson's disease patients with mild cognitive impairment. *Neurosci Lett*. 741:135507.

Liepelt-Scarfone I, Graeber S, Feseker A, Baysal G, Godau J, Gaenslen A, Maetzler W, Berg D. 2011. Influence of different cut-off values on the diagnosis of mild cognitive impairment in Parkinson's disease. *Parkinsons Dis*. 2011:540843.

Litvan I, Goldman JG, Troster AI, Schmand BA, Weintraub D, Petersen RC, Mollenhauer B, Adler CH, Marder K, Williams-Gray CH, et al. 2012. Diagnostic criteria for mild cognitive impairment in Parkinson's disease: movement disorder society task force guidelines. *Mov Disord*. 27:349–356.

Lopes R, Delmaire C, Defebvre L, Moonen AJ, Duits AA, Hofman P, Leentjens AF, Dujardin K. 2017. Cognitive phenotypes in parkinson's disease differ in terms of brain-network organization and connectivity. *Hum Brain Mapp*. 38:1604–1621.

Lui S, Zhou XJ, Sweeney JA, Gong Q. 2016. Psychoradiology: the frontier of neuroimaging in psychiatry. *Radiology*. 281:357–372.

Ma Q, Tang Y, Wang F, Liao X, Jiang X, Wei S, Mechelli A, He Y, Xia M. 2020. Transdiagnostic dysfunctions in brain modules across patients with schizophrenia, bipolar disorder, and major depressive disorder: a connectome-based study. *Schizophr Bull*. 46: 699–712.

Meunier D, Lambiotte R, Bullmore ET. 2010. Modular and hierarchically modular organization of brain networks. *Front Neurosci*. 4:200.

Mijalkov M, Kakaei E, Pereira JB, Westman E, Volpe G, AsD N. 2017. BRAPH: a graph theory software for the analysis of brain connectivity. *PLoS One*. 12:e0178798.

Newman ME. 2006. Modularity and community structure in networks. *Proc Natl Acad Sci U S A*. 103:8577–8582.

Pan N, Wang S, Zhao Y, Lai H, Qin K, Li J, Biswal BB, Sweeney JA, Gong Q. 2021. Brain gray matter structures associated with trait impulsivity: a systematic review and voxel-based meta-analysis. *Hum Brain Mapp*. 42:2214–2235.

Pedersen KF, Larsen JP, Tysnes OB, Alves G. 2017. Natural course of mild cognitive impairment in Parkinson disease: a 5-year population-based study. *Neurology*. 88:767–774.

Pereira JB, Aarsland D, Ginestet CE, Lebedev AV, Wahlund LO, Simmons A, Volpe G, Westman E. 2015. Aberrant cerebral network topology and mild cognitive impairment in early Parkinson's disease. *Hum Brain Mapp*. 36:2980–2995.

Power JD, Barnes KA, Snyder AZ, Schlaggar BL, Petersen SE. 2012. Spurious but systematic correlations in functional connectivity MRI networks arise from subject motion. *NeuroImage*. 59: 2142–2154.

Power JD, Mitra A, Laumann TO, Snyder AZ, Schlaggar BL, Petersen SE. 2014. Methods to detect, characterize, and remove motion artifact in resting state fMRI. *NeuroImage*. 84:320–341.

Sporns O, Tononi G, Kotter R. 2005. The human connectome: a structural description of the human brain. *PLoS Comput Biol*. 1:e42.

Sreenivasan K, Mishra V, Bird C, Zhuang XW, Yang ZS, Cordes D, Walsh RR. 2019. Altered functional network topology correlates with clinical measures in very early-stage, drug-naive Parkinson's disease. *Parkinsonism Relat Disord*. 62:3–9.

Sun H, Lui S, Yao L, Deng W, Xiao Y, Zhang W, Huang X, Hu J, Bi F, Li T, et al. 2015. Two patterns of white matter abnormalities in medication-naive patients with first-episode schizophrenia revealed by diffusion tensor imaging and cluster analysis. *JAMA Psychiatry*. 72:678–686.

Suo X, Lei D, Li N, Cheng L, Chen F, Wang M, Kemp GJ, Peng R, Gong Q. 2017. Functional brain connectome and its relation to Hoehn and Yahr stage in Parkinson disease. *Radiology*. 285:904–913.

Suo X, Lei D, Li L, Li W, Dai J, Wang S, He M, Zhu H, Kemp GJ, Gong Q. 2018. Psychoradiological patterns of small-world properties and a systematic review of connectome studies of patients with 6 major psychiatric disorders. *J Psychiatry Neurosci*. 43:170214.

Suo X, Lei D, Cheng L, Li N, Zuo P, Wang DJJ, Huang X, Lui S, Kemp GJ, Peng R, et al. 2019. Multidelay multiparametric arterial spin labeling perfusion MRI and mild cognitive impairment in early stage Parkinson's disease. *Hum Brain Mapp*. 40:1317–1327.

Suo X, Lei D, Li N, Li W, Kemp GJ, Sweeney JA, Peng R, Gong Q. 2021. Disrupted morphological grey matter networks in early-stage Parkinson's disease. *Brain Struct Funct*. 226:1389–1403.

Suo X, Lei D, Li N, Li J, Peng J, Li W, Yang J, Qin K, Kemp GJ, Peng R, et al. 2021. Topologically convergent and divergent morphological gray matter networks in early-stage Parkinson's disease with and without mild cognitive impairment. *Hum Brain Mapp*. 42: 5101–5112.

Suo X, Lei D, Li W, Li L, Dai J, Wang S, Li N, Cheng L, Peng R, Kemp GJ, et al. 2021. Altered white matter microarchitecture in Parkinson's disease: a voxel-based meta-analysis of diffusion tensor imaging studies. *Front Med*. 15:125–138.

Suo X, Lei D, Li W, Sun H, Qin K, Yang J, Li L, Kemp GJ, Gong Q. 2022. Psychoradiological abnormalities in treatment-naive noncomorbid patients with posttraumatic stress disorder. *Depress Anxiety*. 39:83–91.

Tuovinen N, Seppi K, de Pasquale F, Muller C, Nocker M, Schocke M, Gizewski ER, Kremser C, Wenning GK, Poewe W, et al. 2018. The reorganization of functional architecture in the early-stages of Parkinson's disease. *Parkinsonism Relat Disord*. 50:61–68.

Tzourio-Mazoyer N, Landeau B, Papathanassiou D, Crivello F, Etard O, Delcroix N, Mazoyer B, Joliot M. 2002. Automated anatomical labeling of activations in SPM using a macroscopic anatomical parcellation of the MNI MRI single-subject brain. *NeuroImage*. 15: 273–289.

Wang J, Zuo X, Gohel S, Milham M, Biswal B, He Y. 2011. Graph theoretical analysis of functional brain networks: test-retest evaluation on short- and long-term resting-state functional MRI data. *PLoS One*. 6:e21976.

Wang J, Zuo X, Dai Z, Xia M, Zhao Z, Zhao X, Jia J, Han Y, He Y. 2013. Disrupted functional brain connectome in individuals at risk for Alzheimer's disease. *Biol Psychiatry*. 73:472–481.

Wang J, Wang X, Xia M, Liao X, Evans A, He Y. 2015. GRETNA: a graph theoretical network analysis toolbox for imaging connectomics. *Front Hum Neurosci*. 9:386.

Watts DJ, Strogatz SH. 1998. Collective dynamics of 'small-world' networks. *Nature*. 393:440–442.

Xu X, Guan X, Guo T, Zeng Q, Ye R, Wang J, Zhong J, Xuan M, Gu Q, Huang P, et al. 2018. Brain atrophy and reorganization of structural network in Parkinson's disease with Hemiparkinsonism. *Front Hum Neurosci*. 12:117.

Yan CG, Cheung B, Kelly C, Colcombe S, Craddock RC, Di Martino A, Li Q, Zuo XN, Castellanos FX, Milham MP. 2013. A comprehensive assessment of regional variation in the impact of head micromovements on functional connectomics. *NeuroImage*. 76: 183–201.

Zhang J, Wang J, Wu Q, Kuang W, Huang X, He Y, Gong Q. 2011. Disrupted brain connectivity networks in drug-naive, first-episode major depressive disorder. *Biol Psychiatry*. 70:334–342.